

We are IntechOpen, the world's leading publisher of Open Access books Built by scientists, for scientists

6,900

Open access books available

186,000

International authors and editors

200M

Downloads

Our authors are among the

154

Countries delivered to

TOP 1%

most cited scientists

12.2%

Contributors from top 500 universities



WEB OF SCIENCE™

Selection of our books indexed in the Book Citation Index
in Web of Science™ Core Collection (BKCI)

Interested in publishing with us?
Contact book.department@intechopen.com

Numbers displayed above are based on latest data collected.
For more information visit www.intechopen.com



Theoretical Analysis of the Spectral Photocurrent Distribution of Semiconductors

Bruno Ullrich and Haowen Xi

Additional information is available at the end of the chapter

<http://dx.doi.org/10.5772/51412>

1. Introduction

Measurements of semiconductor photocurrent (PC) spectra have a long and rich history. During the 1960s and 1970s, the topic became one of the most studied phenomena in semiconductor research so that entire textbooks were dedicated to the subject [1-4]. In spite these considerable activities, only a few theoretical efforts were published in order to fit PC spectra. The first attempt is attributed to DeVore [5], who, with the purpose to find an explanation for the typically measured PC peak in the vicinity of the band gap, presumed enhanced carrier recombinations at the semiconductor surface with respect to the bulk. In other words, along the light propagating coordinate the carrier lifetime (and therefore the recombination rate) is changing. However, instead to transfer this idea directly into a mathematical model, DeVore used the non-measurable parameter carrier surface recombination velocity in order to achieve PC fits with a peak.

Much more recently, investigating the PC of thin-film Bi_2S_3 , Kebbab et al. and Pejova reported that the photoconductivity peak cannot be explained using the DeVore model [6-8], while, on the other hand, Pejova noticed that the PC formula published by Bouchenaki, Ullrich et al. (BU model hereafter) in 1991 [9] fits the measured spectra very well. The expression in Ref. [9] was intuitively derived and does not use surface recombination velocity but indeed different recombination rates at the surface and the bulk by introducing different carrier lifetimes along the propagation coordinate of the impinging light. Besides the above mentioned references, Ullrich's formula was successfully employed to fit PC spectra of thin-film CdS [9,10], GaAs [11], ZnS [12] and of the non-common semiconductor YBCO_6 [13].

Considering its correctness for a vast variety of semiconductors, we present here a precise derivation of the BU model and, using bulk CdS as representative semiconducting material, the work reveals the identical excellent agreement between PC experiments and theory for

both: Experimental absorption data and absorption coefficient calculations by combination of density of states and modified Urbach rule [14]. The work further stresses the correct link between the here promoted PC model and the actually measured surface to bulk lifetime ratio, and presents an extended and more detailed manuscript based on our recently published paper [15].

2. General Theory

2.1. Fundamental Equations

The sample geometry for the experiments and theoretical analysis is shown in Fig. 1. The impinging light intensity along the z-axis is I_0 [in J/(s cm²)], and $n(x, y, z, t)$, $p(x, y, z, t)$ are the nonequilibrium electron and hole densities [in 1/cm³], respectively, generated by the incoming photons. The continuity equations are expressed by their general form,

$$\frac{\partial n}{\partial t} = +\frac{1}{e} \nabla \cdot \vec{j}_n - \frac{n}{\tau_n} + \eta \frac{I_0}{\hbar \omega} \alpha \exp(-\alpha z) \quad (1)$$

$$\frac{\partial p}{\partial t} = -\frac{1}{e} \nabla \cdot \vec{j}_p - \frac{p}{\tau_p} + \eta \frac{I_0}{\hbar \omega} \alpha \exp(-\alpha z) \quad (2)$$

where the terms n/τ_n and p/τ_p represent the recombination rates for the electrons and holes, and τ_n and τ_p as their respective lifetimes. The term $I_0/(\hbar \omega) \alpha \exp(-\alpha z)$ is the decay of the generation rate [in 1/(s cm²)] along the penetration of light of the nonequilibrium carriers, where $\hbar \omega$ is the impinging light energy and α is the absorption coefficient [in 1/cm], η is the unit less conversion efficiency coefficient, and e the elementary charge. The vectors \vec{j}_n and \vec{j}_p are the electron and hole components of the current density and are given by,

$$\vec{j}_n = \vec{j}_{n,E} + \vec{j}_{n,D} = eN\mu_n\vec{E} + eD_e\nabla n \quad (3)$$

$$\vec{j}_p = \vec{j}_{p,E} + \vec{j}_{p,D} = eP\mu_p\vec{E} - eD_h\nabla p \quad (4)$$

where $\vec{j}_{n,D}$, $\vec{j}_{p,D}$ stands for the diffusion current driven by the density gradient and $\vec{j}_{n,E}$, $\vec{j}_{p,E}$ represents the conduction current driven by an external electric field \vec{E} . The terms $D_e\nabla n$ and $D_h\nabla p$ refers to the diffusion of the non-equilibrium carriers, whereas D_e and D_h is the diffusion constant of electrons and holes, respectively. The drift mobility of electrons and holes is μ_n and μ_p , and the total electron and hole densities are N and P , which are given by

$$N = N_0 + n \quad (5)$$

$$P = P_0 + p \quad (6)$$

where N_0 and P_0 are the electron and hole equilibrium uniform densities. Hence, the total current density is given by the sum of Esq. (3) and (4),

$$\vec{j} = \vec{j}_n + \vec{j}_p = e(N\mu_n + P\mu_p)\vec{E} + e(D_e\nabla n - D_h\nabla p) \quad (7)$$

We may decompose now Eq. (7) in the total current density \vec{j} in terms of dark current density \vec{j}_{dark} , i.e., current in absence of illumination, and the PC density \vec{j}_{ph} , which is the current generated by the impinging light on the semiconductor,

$$\vec{j} = \vec{j}_{dark} + \vec{j}_{ph} \quad (8)$$

where,

$$\vec{j}_{dark} = e(N_0\mu_n + P_0\mu_p)\vec{E} \quad (9)$$

and

$$\vec{j}_{ph} = e(n\mu_n + p\mu_p)\vec{E} + e(D_e\nabla n - D_h\nabla p) \quad (10)$$

We now assume (i) local neutrality condition, i.e., $n=p$, which implies equal lifetimes of electrons and holes, $\tau_n=\tau_p=\tau$. (ii) the equilibrium electron and hole density N_0 and P_0 are uniform and time independent, i.e., $\partial N_0/\partial t=\partial P_0/\partial t = \nabla N_0=\nabla P_0=0$, and (iii) $\nabla \cdot \vec{E}=0$ under local neutrality condition. With the substitution of the current density \vec{j}_n, \vec{j}_p into Eqs. (1) and (2), we obtain:

$$\frac{\partial n}{\partial t} = +D_e\nabla^2 n - \frac{n}{\tau} + \eta \frac{I_0}{\hbar\omega} \alpha \exp(-\alpha z) + \mu_n \vec{E} \cdot \nabla n \quad (11)$$

$$\frac{\partial p}{\partial t} = +D_h\nabla^2 p - \frac{p}{\tau} + \eta \frac{I_0}{\hbar\omega} \alpha \exp(-\alpha z) - \mu_p \vec{E} \cdot \nabla p \quad (12)$$

We multiply now Eq. (11) and Eq. (12) with the hole and electron conductivity, i.e., σ_p and σ_n , respectively, and, by adding both equations and simultaneously replacing p with n (n=p), we obtain the following relationship:

$$\frac{\partial n}{\partial t} = \frac{\sigma_p D_e + \sigma_n D_h}{\sigma_n + \sigma_p} \nabla^2 n - \frac{n}{\tau} + \eta \frac{I_0}{\hbar \omega} \alpha \exp(-\alpha z) + \frac{\mu_n \sigma_p - \mu_p \sigma_n}{\sigma_n + \sigma_p} \vec{E} \cdot \nabla n \quad (13)$$

Furthermore, we define the bipolar diffusion coefficient as,

$$D = \frac{\sigma_p D_e + \sigma_n D_h}{\sigma_n + \sigma_p} \quad (14)$$

and the bipolar drift mobility μ_E as,

$$\mu_E = \frac{\mu_n \sigma_p - \mu_p \sigma_n}{\sigma_n + \sigma_p} \quad (15)$$

Note that the bipolar drift mobility μ_E is different from the bipolar diffusion mobility μ_D , which is defined as

$$\mu_D = \frac{\mu_n \sigma_p + \mu_p \sigma_n}{\sigma_n + \sigma_p} \quad (16)$$

Thus, we have the continuity equation for n (and consequently for p, because n=p),

$$\frac{\partial n}{\partial t} = D \nabla^2 n - \frac{n}{\tau} + \frac{\eta I_0}{\hbar \omega} \alpha \exp(-\alpha z) + \mu_E \vec{E} \cdot \nabla n \quad (17)$$

and for the PC density:

$$\vec{j}_{ph} = e(\mu_n + \mu_p)n\vec{E} + e(D_e - D_h)\nabla n \quad (18)$$

The Eqs. (17) and (18) are the fundamental equations that allow us, in case the energy dispersion of α is known, to calculate the distribution of the carrier density, carrier current, and the PC spectra.

2.2. Photocurrent spectra for experimental setup condition

So far, we have made some general assumption regarding the process of nonequilibrium carriers. We shall now restrict ourselves to the detailed determination of PC spectra, considering the following general conditions:

- i. stationary state, i.e., $\partial n/\partial t=0$,
- ii. the light illuminates uniformly the entire semiconductor sample, whereas the direction of the impinging light is along the z-axis and the volume of the sample is given by $l_x \times l_y \times l_z$, where $l_z=d$ is the thickness of the sample,
- iii. the sample possesses a uniform nonequilibrium carrier density in the x-y plane, and diffusion takes place along the z-axis only, i.e., $n(x, y, z)=n(z)$, and
- iv. (iv) the external electric field \vec{E} applied to the sample is perpendicular to the incident light and along x-direction, i.e., $\vec{E}=E_x \vec{e}_x$. Hence, with the stationary continuity equation (Eq. 17), we get,

$$D \frac{d^2 n}{dz^2} - \frac{n}{\tau} + \eta \frac{I_0}{\hbar \omega} \alpha \exp(-\alpha z) = 0 \quad (19)$$

In Eq. (19), we have dropped the term $\vec{E} \cdot \nabla n=0$ due to the fact that the two vectors are perpendicular to each other.

In the following step we introduce the boundary condition for solving Eq. (19). Since the PC is measured along the x-axis, i.e., the external electric field is perpendicular to the direction of the impinging light as shown in Fig. 1, consequently, no closed current loop exists in the z-direction. In other words, no physical carrier diffusion current j_D will take place at the boundary $z=0$ and $z=d$. From Eq. (18), we arrive at the boundary conditions,

$$\left. \frac{dn}{dz} \right|_{z=0} = 0 \quad \text{and} \quad \left. \frac{dn}{dz} \right|_{z=d} = 0 \quad (20)$$

By using Eq. (18), we can obtain the PC passing through the sample as $I_{ph} = \iint \vec{j}_{ph} \cdot d\vec{A}$. Here, the electrical current cross-section area vector $d\vec{A}$ is given by $d\vec{A}=dzdy\vec{e}_x$. Notice that the vector $d\vec{A}$ is perpendicular to the cross-section area vector $(D_e - D_h)\nabla n$. Therefore, the diffusion current term $\nabla n=(dn/dz)\vec{e}_z$ in Eq. (18) which is along z-direction does not contribute to the PC. Finally, we obtain the PC for the specific experimental setup as,

$$I_{\text{ph}} = \left(\frac{l_y}{l_x}\right)(\Delta U e \mu) \int_0^d n(z) dz \quad (21)$$

where $\mu = \mu_n + \mu_p$ is the mobility and $\Delta U = E_x l_x$ and the voltage drop across the sample. It is worthwhile noting that I_{ph} has the physical unit of Ampere (A). Equations (19-21), the energy dependence of the absorption coefficient [$\alpha(\hbar\omega)$], and the spatial lifetime distribution of carriers (τ) form the complete set needed for the fit of PC spectra measured with the configuration displayed in Fig. 1.

3. DeVore's approach vs. BU model

In this section, we present the comparison of the two existing theoretical PC models, which were initially introduced in Refs. [5] and [9]. The PC spectra are based on the common experimental setup shown in Fig.1, where the direction of the applied electric field is perpendicular to the direction of illumination.

3.1. The DeVore's photocurrent spectral theory

It has been the conventional way of engage DeVore's formula to fit PC spectra. However, as presented below, for the standard PC experiments displayed in Fig 1, DeVore's formula is actually not the correct one to use. We now briefly outline DeVore's early work [5], in which th calculation is based on the following equation,

$$\frac{1}{\tau\beta^2} \frac{d^2n}{dz^2} - \frac{n}{\tau} + \eta \frac{I_0}{\hbar\omega} \alpha \exp(-\alpha z) = 0 \quad (22)$$

This formulation is based on four assumptions:

- i. the external electric field is perpendicular to the incident light direction, which corresponds the experimental configuration in Fig. 1 (additional discussions of this point will be presented in a forthcoming paper).
- ii. Assuming steady state, i.e., $\partial n/\partial t=0$.
- iii. The recombination rate $1/\tau$ and diffusion length β^{-1} are a constant.
- iv. The recombination current at the surface is given by setting the following boundary conditions:

$$-\frac{1}{\tau\beta^2} \frac{\partial n}{\partial z} \Big|_{z=0} = -n \Big|_{z=0} S \quad \text{and} \quad -\frac{1}{\tau\beta^2} \frac{\partial n}{\partial z} \Big|_{z=d} = +n \Big|_{z=d} S \quad (23)$$

Where the constant S is called surface recombination velocity. By solving the standard second order differential equation $n(z)$ with the boundary conditions [Eq. (22)], and substitute $n(z)$ into the expression of I_{ph} [Eq. (21)], we arrive at DeVore's formula,

$$I_{ph} = I_{PC}^0 F \tag{24}$$

where the PC magnitude is given by,

$$I_{ph}^0 = \left(\frac{l_y}{l_x}\right)(\Delta U e \mu) \left(\tau \frac{I_0}{\hbar \omega}\right) \tag{25}$$

and the dimensionless spectrum factor F has the form,

$$F = \frac{1}{1 - \alpha^2 / \beta^2} \left[1 - \exp(-\alpha d) - \frac{\alpha S \tau (1 + \exp(-\alpha d) + \alpha^2 \beta^2 (1 - \exp(-\alpha d)))}{1 + S \tau \beta \coth(\beta d / 2)} \right] \tag{26}$$

where α is the energy dependent absorption coefficient. We argue that the boundary conditions [Eq. (22)] are not consistent with the experimental setup, i.e. the PC is driven by an applied electric field, which is perpendicular to the impinging light. Therefore, at the surface along the incident light there is an open circuit. The correct boundary condition is that there will be no particle current across the sample surface, i.e., $-\frac{1}{\tau \beta^2} \frac{\partial n}{\partial z} \Big|_{z=0} = -\frac{1}{\tau \beta^2} \frac{\partial n}{\partial z} \Big|_{z=d} = 0$. Under this boundary condition, the DeVore's PC becomes,

$$I_{ph} = I_{PC}^0 [1 - \exp(-\alpha d)] \tag{27}$$

i.e., the spectral factor F in Eq. (25) is reduced to the absorption,

$$F = 1 - \exp(-\alpha d) \tag{28}$$

Consequently, DeVore's formula is not able to explain the PC maximum in the vicinity of the band gap for the geometry shown in Fig. 1. The boundary conditions expressed by Eq. (22) are artificially acting as source of non-equilibrium carriers.

3.2. PC theory based on the spatial non-uniform recombination rate (BU model)

The ansatz of the original BU model in Ref. [9] led to an intuitive and straightforward theory that implemented DeVore's assumption directly. It simply assumed that the spatial distribu-

tion recombination rates along the light propagation - i.e., at the surface and in the bulk region - are different. At the surface, due to the increased density of recombination centers with respect to the bulk, the carrier lifetime is much shorter than in the bulk region. Specifically, it was assumed that the spatial lifetime decay $\tau(z)$ takes the simple form:

$$\tau(z) = \tau_b \left[1 - \left(1 - \frac{\tau_s}{\tau_b} \right) \exp(-z/L) \right] \quad (29)$$

Where τ_s is the lifetime of the nonequilibrium carriers at the surface, τ_b is the lifetime of the nonequilibrium carriers in the bulk, and L is the length scale beyond which the recombination rate is predominately ruled by τ_b . Thus we have a multi-time scale relaxation model. We rearrange Eq. (19), resulting in,

$$n = \frac{1}{\beta^2} \frac{d^2 n}{dz^2} + \tau \eta \frac{I_0}{\hbar \omega} \alpha \exp(-\alpha z) \quad (30)$$

Here, we have used the mean field approximation for the term $D\tau \approx D\langle\tau\rangle = 1/\beta^2$ and assumed that diffusion length β^{-1} is a constant. We now substitute Eq. (30) into the general PC expression Eq. (21), we find,

$$I_{ph} = \left(\frac{l_y}{l_x} \right) (\Delta U e \mu) \int_0^d \left(\frac{1}{\beta^2} \frac{d^2 n}{dz^2} + \tau(z) \eta \frac{I_0}{\hbar \omega} \alpha \exp(-\alpha z) \right) dz = I_{ph}^0 F \quad (31)$$

The first integral over the diffusion term is zero because of the zero flux boundary condition [Eq. (20)]. Thus, the dimensionless spectrum factor F takes the following form:

$$F = \int_0^d \frac{\tau(z)}{\tau_b} \alpha \exp(-\alpha z) dz = 1 - \exp(-\alpha d) - \left(1 - \frac{\tau_s}{\tau_b} \right) \frac{\alpha L}{1 + \alpha L} [1 - \exp(-\alpha d - d/L)] \quad (32)$$

where, the PC magnitude is given by,

$$I_{ph}^0 = \left(\frac{l_y}{l_x} \right) (\Delta U e \mu) \left(\frac{I_0}{\hbar \omega} \tau_b \right) \eta \quad (33)$$

Equations (31-33) basically correspond to the intuitively deduced PC dispersion Ref. [9]. We note that by expressing the PC in terms of the responsivity (R) in [Ampere/Watt], i.e., for constant impinging light power, the proportionality $R \propto F$ holds.

4. Experimental PC Results and Fits

The spectral PC dispersion was investigated by using the experimental arrangement in Fig. 1: The x, y plane of the CdS bulk material faces the incoming monochromatic light, while the z coordinate is parallel to the light propagation. The electric field of the light is perpendicularly oriented to the c -axis of the CdS sample, which was an industrially produced single crystal with $d=1$ mm. Two vacuum evaporated Al contacts with a gap of 0.5 mm between them were used for the electrical connection. The applied electric field driving the PC was 200 V/cm and the optical excitation was carried out with intensities typically in $\mu\text{W}/\text{cm}^2$ range. The PC was recorded at room temperature with lock-in technique by chopping the impinging light at 25 Hz. The measured spectrum was corrected by a calibrated Si photodiode in order to express the PC in terms of responsivity.

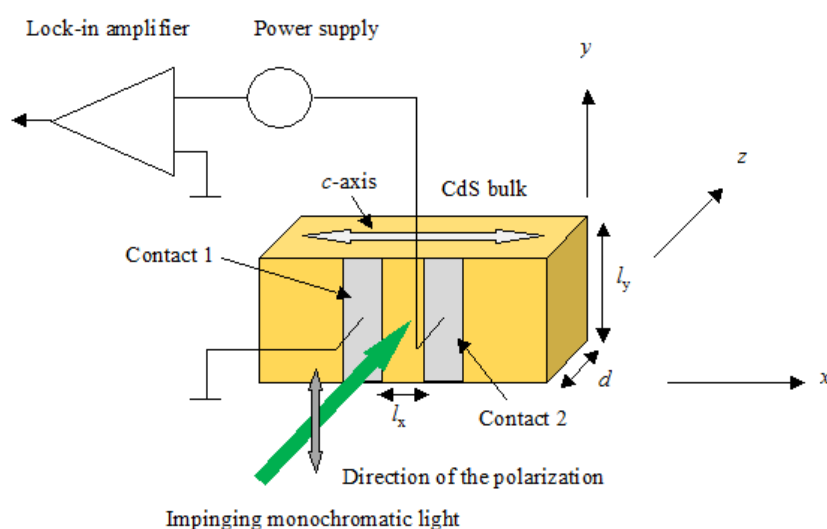


Figure 1. Experimental arrangement employed for the experiments. Note that $d=l_z$.

4.1. PC fit using Dutton's experimentally determined absorption coefficient

The comparison of the experiment (symbols) with the fit (dotted line) using Eq. (31-32) is shown in Fig. 2(a). The best fit between the experimental data and theoretical formula was achieved with $d=3.60 \times 10^{-3}$ cm, $L=8.65 \times 10^{-5}$ cm, and $\tau_s/\tau_b=0.068$, while the used $\alpha(\omega\hbar)$ values, which are shown in Fig. 2 (b), have been extracted from Dutton's paper [16]. The fit reveals that only an effective thickness of the sample, which does not necessarily correspond to the physical thickness, contribute to the formation of the PC signal. The corresponding conclusion was found by analyzing the photoluminescence of thin-film CdS [17].

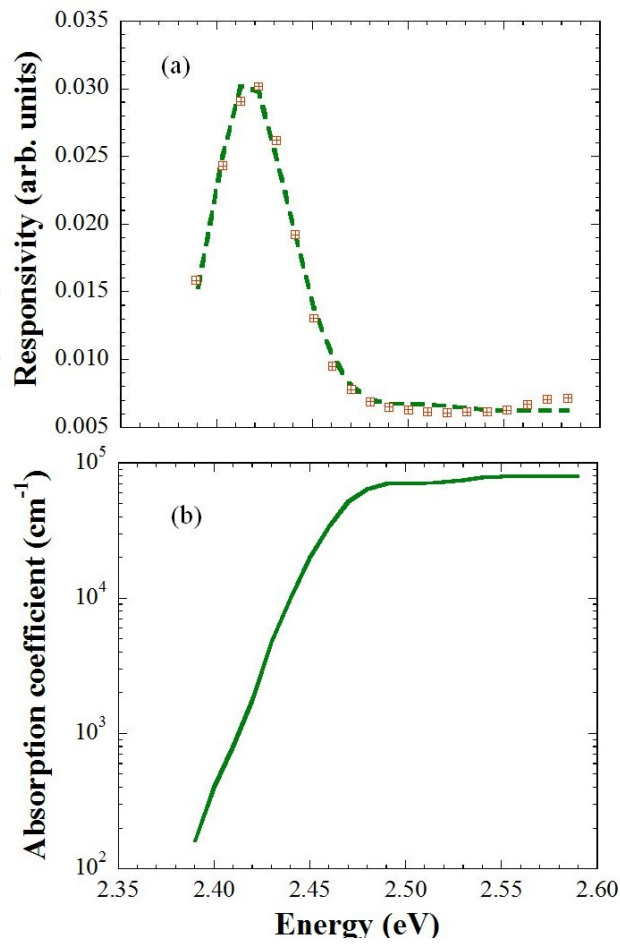


Figure 2. a) The symbols represent the photocurrent measurements while the broken line was fitted with the Eq. (32). (b) The absorption coefficient for perpendicularly oriented CdS was used for the fit. The data were deduced from Dut-ton’s paper (Ref. [16]).

Using Eq. (32) one can link the absorption coefficient to the location of the maximum of the PC spectra. We set $\frac{dF}{d\hbar\omega} = \frac{dF}{d\alpha} \frac{d\alpha}{d\hbar\omega} = 0$, and obtain,

$$d \exp(-\alpha d) - \left(1 - \frac{\tau_s}{\tau_b}\right) \left[\frac{L}{(1 + \alpha L)^2} (1 - \exp(-\alpha d - d/L)) + \frac{\alpha L}{(1 + \alpha L)} d \exp(-\alpha d - d/L) \right] = 0$$

Since the term $\exp(-\alpha d - d/L) \ll 1$, we simplify the above condition to,

$$d \exp(-\alpha d) - \left(1 - \frac{\tau_s}{\tau_b}\right) \frac{L}{(1 + \alpha L)^2} = 0 \tag{34}$$

resulting in $-\alpha d = \ln\left(1 - \frac{\tau_s}{\tau_b}\right) \frac{L}{d} - 2\ln(1 + \alpha L) = 0$ and by using the approximation $\ln(1 + \alpha L) \approx \alpha L$ and $L/d \ll 1$, we finally find the α^* where the PC has the maximum value

$$\alpha^* d = -\ln\left(\left(1 - \frac{\tau_s}{\tau_b}\right) \frac{L}{d}\right) \left(\frac{1}{1 - 2L/d}\right) \cong -\ln\left(\left(1 - \frac{\tau_s}{\tau_b}\right) \frac{L}{d}\right) \quad (35)$$

This shows that the maximum location ($\alpha^* d$) in PC spectra is mainly controlled by two parameters τ_s/τ_b , L/d . Now we substitute the parameters $d=3.60 \times 10^{-3}$ cm, $L=8.65 \times 10^{-5}$ cm, and $\tau_s/\tau_b=0.068$ into α^* expression, we obtain $\alpha^*=1108.54$ cm⁻¹. This corresponds to the energy E value between 2.41eV-2.42eV, and is exactly the energy region where the maximum PC occurred.

4.2. PC fit employing the theoretical absorption coefficient based on the modified Urbach rule

So far, we have used the experimental absorption edge data from Dutton directly, we may also fit the PC by modeling $\alpha(\hbar\omega)$ with the density of states and the modified Urbach tail, which are expressed by [14],

$$\begin{aligned} \alpha(\hbar\omega) &= A_0 \sqrt{\hbar\omega - E_g} \\ \text{if} & \\ \hbar\omega &\geq E_{cr} \end{aligned} \quad (36)$$

and

$$\begin{aligned} \alpha(\hbar\omega) &= A_0 \sqrt{\frac{kT}{2\sigma}} \exp\left[\frac{\sigma}{kT} (\hbar\omega - E_{cr})\right] \\ \text{if} & \\ \hbar\omega &\leq E_{cr} \end{aligned} \quad (37)$$

where E_g is band gap energy, A_0 is linked to the saturation value of $\alpha(\hbar\omega)$, kT is the thermal energy, and the crossover between Eqs. (36) and (37) takes place at $E_{cr}=E_g+kT/(2\sigma)$ [14], where σ defines the steepness of the Urbach tail [17]. Figure 3 shows the comparison of the measured PC [which is identical with the one in Fig. 2 (a)] with the fit using Eq. (32), (36), and (37), whereas the following fitting parameters were used: $kT=26$ meV, $A_0=3.26 \times 10^5$ cm⁻¹ (eV)^{-1/2}, $d=3.69 \times 10^{-3}$ cm, $L=9.14 \times 10^{-5}$ cm, $\sigma=2.15$, $E_g=2.445$ eV, and $\tau_s/\tau_b=0.100$. The fit parameters d and L are very close to the previous fit and we should stress that the σ value found ($=2.15$) is almost identical with the promoted CdS value ($=2.17$) of Dutton. Figure 4 shows the comparison of the calculated function $\alpha(\hbar\omega)$ with Dutton's measurement and the good agreement of both curves proves the suitability of the straightforward concept represented by Eq. (35) and (36).

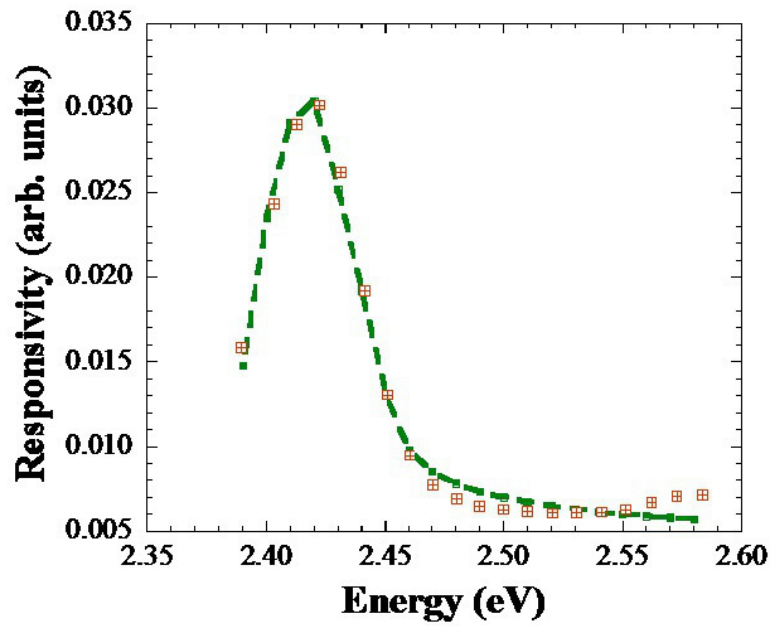


Figure 3. Fit (broken line) of the measured photocurrent spectrum in Fig. 1 (symbols) using Eqs. (36) and (37). The fit hardly differs from the one in Fig. 2 (a).

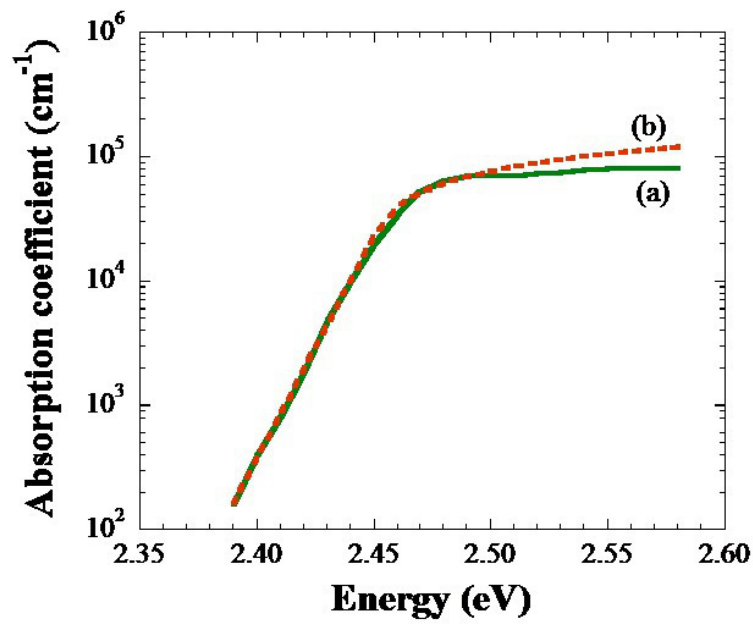


Figure 4. Comparison of the absorption coefficient (a) after Dutton and (b) modeled with Eqs. (36) and (37).

5. Measurement of the lifetime at the surface (τ_s) and in the bulk (τ_b)

By measuring the temporal decay of the PC illuminating the sample with highly ($\alpha(\hbar\omega)=10^5 \text{ cm}^{-1}$) and less absorbed light ($\alpha(\hbar\omega)\ll 10^2 \text{ cm}^{-1}$) it should be possible to measure τ_s and τ_b . We made the temporal PC decay visible with a 500 MHz scope by employing chopped (18 Hz) continuous wave (cw) laser beams at 488.0 nm (2.54 eV) and 632.8 nm (1.96 eV), by using an Ar-Kr and He-Ne laser, respectively. Both laser beams were unfocused resulting in the rather moderate intensity of about 0.6 W/cm^2 and, as for the PC measurements above, the driving electric field was again 200 V/cm .

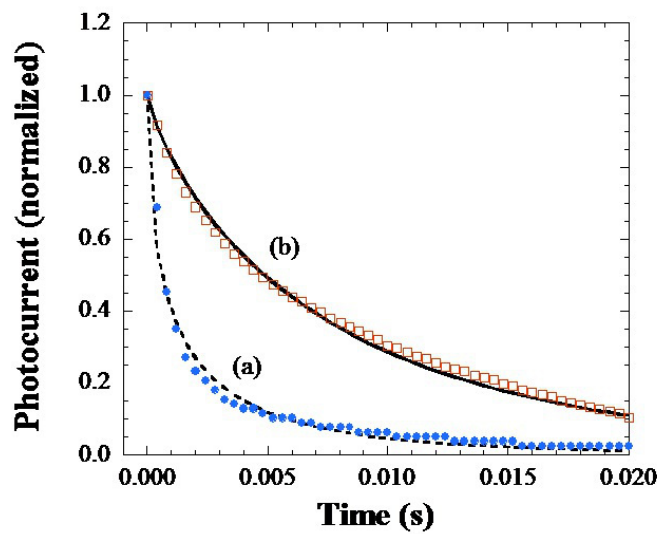


Figure 5. Photocurrent decay vs. time measured under the illumination of a laser emitting at (a) 488.0 nm and (b) 632.8 nm. The symbols represent the measurements, while solid and broken lines represent the fits done with Eq. (38).

Figure 5 shows the experimental results (symbols) and fits (solid and broken lines) of the decay. The fits were performed with the Kohlrausch function [19], which is an extension of the exponential function with one additional parameter γ that can range between 0 and 1,

$$I_{\text{ph}}(t) = I_{\text{ph}}^0 \exp[-(t / \tau_{s,b})^\gamma] \quad (38)$$

The following parameters resulted in the best fits for surface and bulk: $\tau_s=1.2 \text{ ms}$ and $\gamma=0.53$, and $\tau_b=7.6 \text{ ms}$ and $\gamma=0.82$, respectively, resulting in $\tau_s/\tau_b=0.16$. Despite the straightforwardness of the experiment, which did not consider electric charging effects, the number is only approximately a factor 2.4 and 1.6 off from the predicted value using the data of Dutton and the modeled absorption edge, respectively. It is worthwhile to note that the Kohlrausch decay can be expressed as linear superposition of simple exponential decays, i.e.,

$\exp[-(t/\tau_{s,b})^\gamma] = \int_0^\infty p(u, \gamma) \exp[-t/(u\tau_{s,b})] du$, where $p(u, \gamma)$ is the weight function for the decay time $\tau = u\tau_{s,b}$. The mean relaxation time is $\langle \tau \rangle = \int_0^\infty \exp[-(t/\tau_{s,b})^\gamma] dt = \frac{\tau_{s,b}}{\gamma} \Gamma(\frac{1}{\gamma})$, where Γ is the gamma function. For a simple exponential decay, $\langle \tau \rangle = \tau_{s,b}$, and, therefore, the necessity of the Kohlrausch function to fit the temporal PC decay confirms the involvement of various time constants and is strong supportive evidence for the multi-time scale relaxation model introduced by Eq. (29).

6. Conclusion

We have derived a spectral PC formula based on general principles for the standard set-up used in experiments. By explicitly including the spatial variation of the recombination rate along the light propagation - i.e., at the surface and in the bulk region - we were able to demonstrate that PC spectra can be accurately described by the BU model. Equivalently good agreements between theory and experiment were found by using $\alpha(\hbar\omega)$ values either experimentally determined or straightforwardly modeled by the density of states and the modified Urbach rule. Furthermore, we have shown that the detailed theoretical model of the spatial variation of $\tau(z)$ is not critical for the generation of the PC near the band gap. However, the presented detailed theory correctly fit and explains the experimental observations. It reveals the firm physical key mechanism for understanding of the PC peak near the gap energy: The peak takes place due to the different recombination rates of the excited carriers near the surface and bulk. We also showed that the τ_s/τ_b ratio found by temporally resolved PC measurements reasonably agrees with the results from the PC fits, accommodating the commonly used concept in optoelectronics, i.e., the use of carrier lifetimes.

Author details

Bruno Ullrich^{1,2,3*} and Haowen Xi⁴

*Address all correspondence to: bruno.ullrich@yahoo.com

1 Ullrich Photonics LLC, USA

2 Air Force Research Laboratory, Materials & Manufacturing Directorate, Wright Patterson, USA

3 Instituto de Ciencias Físicas, Universidad Nacional Autónoma de México, Cuernavaca, Morelos, México

4 Department of Physics and Astronomy, Bowling Green State University, USA

References

- [1] Bube, R. H. (1960). *Photoconductivity of Solids*. New York:, Wiley.
- [2] Ryvkin, S. M. (1964). *Photoelectric Effects in Semiconductors*. New York:, Consultants Bureau.
- [3] Rose, A. (1978). *Concepts in Photoconductivity and Allied Problems*. New York:, Krieger.
- [4] Mort, J., & Pai, D. M. (1976). *Photoconductivity and Related Phenomena*. Amsterdam, Elsevier.
- [5] DeVore, H. B. (1955). Spectral Distribution of Photoconductivity. *Phys. Rev.*, 102, 86-91.
- [6] Kebbab, Z., Benramdane, Medles. M., Bouzidi, A., & Tabet-Derraz, H. (2002). Optical and Photoelectrical Properties of Bi_2S_3 Thin Films btained by Spray Pyrolysis Technique. *Solar Energy Materials & Solar Cells*, 71, 449-457.
- [7] Pejova, B. (2007). Structural, Optical and Photoelectrical Properties of Low-dimensional Semiconductors deposited in Thin Film Form by Chemical and Sonochemical Methods, in *Progress in Solid State Chemistry Research*. Buckley RW, editor. Nova Science Publishers, New York , 55-115.
- [8] Pejova, B. (2008). Analysis of the Shape of Spectral Dependence of Absorption Coefficient and Stationary Photoconductivity Spectral Response in Nanocrystalline Bismuth (III) Sulfide Thin Films. *Mater. Res. Bull.*, 43, 2887-2903.
- [9] Bouchenaki, C., Ullrich, B., Zielinger, J. P., Cong, H. N., & Chartier, P. (1991). Preparation, Characterization, and Bistable Photoconduction Properties of Thin CdS layers. *J. Opt. Soc. Am. B*, 8(3), 691-700.
- [10] Bouchenaki, C., Ullrich, B., Zielinger, J. P., Cong, H. N., & Chartier, P. (1990). Photoconduction and Thermo-optical Hysteresis Measurements in Thin CdS Films. *J. Crystal Growth*, 101, 797-801.
- [11] Erlacher, A., Ambrico, M., Capozzi, V., Augelli, V., Jaeger, H., & Ullrich, B. (2004). X-ray, Absorption and Photocurrent Properties of Thin-Film GaAs on Glass formed by Pulsed-laser Deposition. *Semicond.Sci. Technol.*, 19, 1322-1324.
- [12] Yano, S, Schroeder, R, Sakai, H, & Ullrich, B. (2003). High-electric-field photocurrent in thin-film ZnS formed by pulsed-laser deposition. *Appl. Phys. Lett.*, 82, 2026.
- [13] Ullrich, B., Kulac, I., & Pint, H. (1992). Photocurrent in Thin $\text{YBa}_2\text{Cu}_3\text{O}_6$ Films on Sapphire. *Jpn. J. Appl. Phys.*, 31, L 856-L859.

- [14] Ullrich, B., & Bouchenaki, C. (1991). Bistable Optical Thin CdS Film Devices: All-optical and Optoelectronic Features. *Jap. J. Appl. Phys.*, 30, L 1285-L1288.
- [15] Ullrich, B., & Xi, H. (2010). Photocurrent Theory based on Coordinate Dependent Lifetime. *Optics Letters*, 35(23), 3910-3912.
- [16] Dutton, D. (1958). Fundamental Absorption Edge in Cadmium Sulfide. *Phys. Rev.*, 112(3), 785-792.
- [17] Ullrich, B., Yano, S., Schroeder, R., & Sakai, H. (2003). Analysis of single- and two-photon-excited green emission spectra of thin-film cadmium sulfide. *J. Appl. Phys.*, 93, 1914-1917.
- [18] Urbach, F. (1953). The Long-Wavelength Edge of Photographic Sensitivity and of the Electronic Absorption of Solids. *Phys. Rev.*, 92, 1324.
- [19] Queisser, H. J. (1985). Nonexponential Relaxation of Conductance near Semiconductor Interfaces. *Phys. Rev. Lett.*, 54, 234-236.